Macromolecules
ARTICLE

Macromolecules **2010**, *43*, 3903–3910 **3903**
DOI: 10.1021/ma100477p

Glass Transitions, Segmental Dynamics, and Friction Coefficients for Individual Polymers in Multicomponent Polymer Systems by Chain-Level Experiments

Lance Gill, Joshua Damron, Marcin Wachowicz, and Jeffery L. White*

Department of Chemistry, Oklahoma State University, Stillwater, Oklahoma 74078

Received March 2, 2010; Revised Manuscript Received March 24, 2010

ABSTRACT: Chain-level details about the behavior of pure PI (polyisoprene) and pure PVE (polyvinylethylene), versus their behavior in the miscible blend with one another, are investigated using chain-specific solid-state NMR experiments over a wide temperature range. The PI/PVE blend is a well-known miscible blend, and we compare previous results to those obtained from the experimental strategy we have recently developed (for evaluating miscibility and configurational entropy in saturated polyolefin blends, e.g., *Macromolecules* **2008**, *41*, 2832 and *Macromolecules* **2007**, *40*, 5433), which employs variable-temperature solid-state magic-angle spinning CODEX NMR experiments to provide chain-specific information for either component in the blend. Even though the PI/PVE blend is miscible, we experimentally verify that the effective glass transitions for each chain type are inequivalent in the blend, and slow segmental dynamics for each polymer in the blend are characterized by unique central correlation times and correlation time distributions. Quantitative analysis of the raw data from the variable-temperature solid-state CODEX NMR methodology indicates that good agreement exists between effective T_g's, central correlation time constants, correlation time distributions, and friction coefficients extracted from this approach versus those obtained by other methods. That such quantitative information may be obtained for either polymer component in an amorphous mixture, without isotopic labeling, electric dipole moment constraints, or introduction of probe molecules, is a unique advantage of this experimental strategy and illustrates applicability to a wide range of mixed macromolecular systems beyond miscible blends, including polymer nanocomposites, organic/inorganic hybrids, biological macromolecules, and block copolymers.

Introduction

Miscible polymer blends present significant challenges to our fundamental understanding of the connections between molecular and macroscopic properties in macromolecular mixtures. While many commercial polymer blend applications exist, their discovery and optimization have essentially followed empirical methods. Recently, the polymer blend literature has addressed deficiencies in the predictive understanding of binary miscible blends by focusing on the temperature and composition dependence of chain dynamics in their mixed and unmixed states, as well as the failure of empirical time−temperature superposition relationships, via a variety of experimental and computational approaches. Key aspects of recent discussions surrounding miscible blends include dynamic heterogeneity,[1,2] different effective glass transitions for the polymer constituents in the blend, particularly for blends whose components have large differences in the T_g's,[3,4] the characteristic minimum length scale for cooperative chain rearrangements,[5,6] local composition variations and the role they play in differential chain behavior, or as stated in the recent language found in the literature, the relative contributions of "self-concentration" and "concentration fluctuations" and the failure of time−temperature superposition.[7−12] A recent review has summarized some of the progress toward addressing many of these key outstanding questions.[13]

Our own recent experimental work, which has relied heavily on advanced solid-state NMR methods, revealed new information regarding the formation of miscible polyolefin blends and their individual segmental dynamics at or near the glass transition temperature.[14−17] Specifically, chain-level experiments on this class of athermal polymer mixtures indicated that (1) configurational entropy can drive mixing in miscible polyolefin blends, (2) the effective T_g's of each polymer component in the miscible blend may or may not be identical and must be evaluated on a case-by-case basis, and (3) dynamic heterogeneity exists and upon formation of a miscible polyolefin blend, the dynamic heterogeneity significantly increases for the high-T_g blend component while the low-T_g blend component experiences much smaller perturbations in chain dynamic heterogeneity. Our previous experiments focused on slow chain dynamics near the glass transition, i.e., segmental dynamics, and did not address terminal dynamics accessed at much higher temperatures. In the course of pursuing direct experimental evidence for why polyolefin blends exhibit such unique mixing behavior, we recognized that the experimental approach utilizing temperature dependent CODEX NMR[18,19] was equally well-suited for addressing many of the larger, general questions surrounding miscible polymer blends as described in the preceding paragraph. Indeed, the experimental approach offers some important advantages that allow general application to any polymer blend or composite system. These advantages include the following: (1) no isotopic labeling is required; (2) no physical modification of the material is required, e.g., solvent or small molecule addition; (3) the individual blend components do not have to have an electric dipole moment, as is required for dielectric spectroscopy (which becomes complicated if both species are dielectrically active); (4) chain-specific resolution takes place even in the blend, unlike typical calorimetric methods; (5) raw data is amenable to treatment using models familiar to the broader polymer science community, including those which capture spatially and temporally heterogeneous chain behavior; (6) the

*Author to whom all correspondence should be addressed. E-mail: jeff.white@okstate.edu.

Published on Web 03/30/2010

ability exists to interrogate chain behavior below, at, or above the glass transition temperature. These advantages have recently been discussed in previous publications for binary blends containing various combinations of polyethylene, atactic polypropylene, polyisobutylene, polyethylene-*co*-butene, and head-to-head polypropylene.[14−17] Here, we discuss recent experimental results and their implications in the context of the larger questions surrounding polymer blend science for the PI (polyisoprene) and PVE (polyvinylethylene or poly-1,2-butadiene) blend, a classic ideal miscible blend whose pure polymers have > 50 K difference in their individual T_g's, and which are known to be intimately mixed when the PVE 1,2-diene content exceeds ca. 85%. We have chosen the PI/PVE blend system (50/50 mol %) as it has been studied extensively by many researchers using a variety of methods and theory,[20−33] including several key ^{2}H labeling wide-line NMR experiments by Kornfield and co-workers that helped generate significant interest in the blend.[34−36] On the basis of this wealth of published data, the PI/PVE blend will serve as an excellent baseline for validating the experimental approach as generally applicable to any mixed polymer or composite system without the aforementioned limitations often encountered with other experimental strategies.

The specific chain-level NMR experiments discussed below for PI/PVE quantitatively reveal (1) the length scales of mixing in the polymer mixture, (2) distinct effective T_g's for each component, (3) central correlation times characteristic of slow segmental dynamics over a wide temperature range (beginning at or below T_g) for each polymer before and after blending, (4) the breadth of the correlation time distribution before and after formation of the miscible blend, and (5) friction coefficients for each blend component before and after blend formation. Agreement exists between our results and previously published results on this blend system. We find that the individual blend components do not exhibit the same effective T_g in the miscible blend, and the high-T_g blend component (PVE) experiences a significantly larger change in its temperature-dependent central correlation time and correlation time distribution (characteristic of slow segmental dynamics) versus the low-T_g PI. These chain-level experiments reinforce the emerging picture of inequivalent individual chain dynamics in miscible polymer blends. Our results will be discussed in detail relative to the extensive literature on this blend system, the comparison of which demonstrates the overall validity of our experimental design as a general strategy for essentially any polymer blend or polymer composite/nanocomposite system from which one can obtain an NMR signal.

Experimental Section

Samples and Data Collection. A commercial polyisoprene (PI) sample was obtained from Aldrich, with MW ~800 000 and microstructure corresponding to 97% *cis*-1,4 enchainment (catalog no. 182141). Polyvinylethylene (PVE) was purchased from Polymer Source, Inc. (catalog no. P390-Bd). The molecular weight and polydispersity index (PDI) was obtained by size exclusion chromatography (SEC) in THF. SEC analysis was performed on a Varian gel-permeation chromatograph equipped with refractive and UV light scattering detectors. The PVE sample has M_w/M_n ratio of 1.04 (M_w = 11450) and 88% 1,2-polybutadiene enchainment. The percent 1,4 enchainment in PVE was calculated using integration of the olefinic region of the ^{13}C single-pulse experiment, yielding 12% 1,4 isomer. Equimolar PI/PVE blends were made via toluene dissolution for 24 h and then mixed for 72 h to form the blend.

Thermal analysis of the samples was completed using a TA Q2000 differential scanning calorimeter (DSC), with a 10 K/min heating rate. The endotherm midpoint from the second heating scan was assigned as the calorimetric glass transition (T_g) temperature. Solid-state NMR $T_{1\rho H}$ measurements confirmed intimate mixing for the blended components, and experimental results were compared to simple mixtures of the same polymers. The experimental DSC and $T_{1\rho H}$ data are reported in Table 1.

Table 1. DSC T_g Values for the Polymers and Blends Acquired Using a 10 K/min Rate, and $T_{1\rho H}$ Measurements Obtained at 230 K. The Pure Polymers have Essentially Identical $T_{1\rho H}$ Values at 198 K

	PI pure	PVE pure	PI blend	PI mixed	PVE blend	PVE mixed
DSC T_g	208 K	263 K	214 K	208 K	224 K	263 K
$T_{1\rho H}$	1.9 ms	13.8 ms	5.1 ms	1.5 ms	6.5 ms	13.1 ms

All ^{13}C and ^{1}H measurements were collected on a Bruker DSX-300 with field strength equal to 7.05T. Solid-state CODEX NMR experiments were performed on a 4 mm double-resonance magic-angle spinning probe using the pulse sequence in Figure 1, previously described in detail by deAzevedo and Schmidt-Rohr.[18,19] The probe temperature was calibrated using $PbNO_3$ to within ±1 K. All CODEX exchange data was acquired with an actively controlled 4.5 kHz MAS speed, a 1 ms cross-polarization contact time, rotor synchronization, and acquisitions were alternated between the exchange and reference signal every 256 scans to eliminate spectrometer drift. All slow exchange data were acquired using a 200 ms exchange time. Total experiment times typically ranged between 8 and 20 h for a single measurement, depending on the temperature.

Experimental Verification of Blend Miscibility. Table 1 shows results from DSC and ^{1}H $T_{1\rho}$ NMR measurements. As expected, the DSC measurements agree with multiple reports in the previous literature; a broad, featureless endotherm was observed for the blend, whereas the mixed sample exhibited distinct individual pure component transitions. Using known spin-diffusion length scale equations, the essentially equivalent ^{1}H $T_{1\rho}$ time constants for the blend (T = 230 K, where spin-diffusion is efficient) indicate miscibility at a length scale of mixing equal to 1.8−2.2 nm, which is significantly smaller than chain dimensions for either polymer component, and indeed on the order of accepted Kuhn lengths for these polymers.[37]

Calculations and Theory. Data analysis methods used for this miscible blend system are the same as applied to the previously published aPP/PEB66 and hhPP/PIB polyolefin systems.[15−17] Complete details are described in the Supporting Information. Chain conformational exchange data from variable temperature CODEX experiments were analyzed to extract correlation time constants, activation energies for chain reorientation, and quantitative correlation time distributions. An isotropic rotational diffusion model (employing 20 discrete conformer populations as an approximation to the heterogeneous backbone conformer distribution) was used to simulate the experimental data and solve the overall equilibrium exchange matrix as a function of the exchange mixing time in the CODEX experiment and the correlation time constant for the specific polymer at each temperature. A discrete log-Gaussian correlation time distribution function was analyzed with respect to temperature using an Arrhenius model, which was also compared to results from a WLF/KWW model analysis of the experimental data. Powder averaged values of the chemical shift anisotropy, reflecting the distribution of tensor orientations in the amorphous polymers, were included in all calculated fits of the data. The *Mathematica* program (version 6.0) was used for all calculations.

Results and Discussion

Exchange Data for Pure PI and PVE. Figure 2 shows representative ^{13}C CODEX NMR spectra for pure PI and PVE, and their blend. The details of the CODEX experiment itself, and the variable temperature strategy used for polymer blends has been discussed extensively in previous contributions.[15−17] In summary, spectra are obtained over the entire temperature range spanning each pure polymer, and

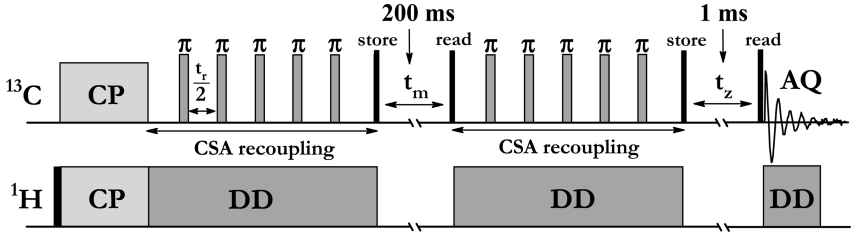

Figure 1. CODEX experiment pulse sequence applied under conditions of MAS. The value of the exchange mixing time t_m = 0.2 s for all data reported in this paper, unless specifically noted. The total CSA evolution time corresponding to the sum of the first and second recoupling period was $2Nt_r$ = (2)(4)(0.22 ms) = 1.76 ms.

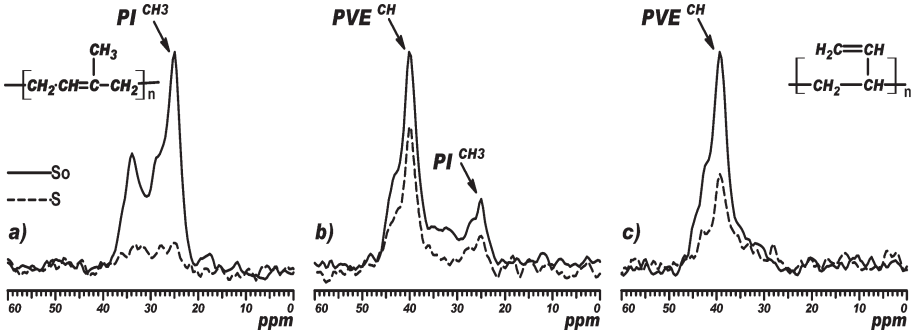

Figure 2. Example ^{13}C CODEX spectra showing only the aliphatic region, from which backbone dynamics were interrogated, for (a) pure PI at 214 K, (b) PI/PVE 50/50 mol % blend at 236 K, and (c) pure PVE at 263 K. The solid line represents the reference spectrum with t_z = 1 ms (S_o) and the dashed line is the CODEX spectrum obtained with t_m = 200 ms (S).

specifically for the PI/PVE system, from 193 to 280 K. The experiment is actually run in duplicate to generate two data sets at each temperature, which differ in that the t_m and t_z periods are interchanged, generating what is known as the exchange spectrum S (t_m and t_z positioned as shown in Figure 1) versus the reference spectrum S_o (no mixing; t_m and t_z switched from that shown in Figure 1).[18,19] The pure exchange spectrum is the difference between these two results, denoted as $\Delta S = S_o - S$. The amplitude of this signal is related to the normalized exchange intensity $E(t_m, \tau_c, T) = \Delta S/S$, as previously discussed,[38] and in addition to the temperature dependence, the amplitude depends on the mixing time t_m and the correlation time τ_c characteristic of segmental dynamics. The mixing time is a real time parameter that can be varied (in practice from a few microseconds to almost one second; in theory up to several seconds if polarization can be preserved). Most importantly for this contribution, systematic comparisons of E as a function of temperature for pure polymers versus the same polymers in the binary blend can reveal quantitative changes in slow chain dynamics and their distributions upon blend formation. As a result, exchange intensity curves as a function of temperature, beginning at or below the known T_g for each component, provide the raw experimental data from which we can extract correlation times and correlation time distributions characteristic of slow segmental chain reorientation for each component in the miscible blend. As stated previously, this is achieved without any isotopic labeling or tracer/probe molecule introduction.

Exchange intensity curves $E(T)$ for 0.2 s mixing times are shown in Figure 3 for the two pure polymers PI and PVE. Qualitatively, the curves provide the expected shape for variable-temperature CODEX experiments, as no exchange intensity is observed at very low temperatures, exchange intensity increases as the temperature increases and polymer segments begin to reorient, and finally at high temperatures, no exchange intensity remains as chain motion becomes fast enough to isotropically average the chemical shift anisotropy

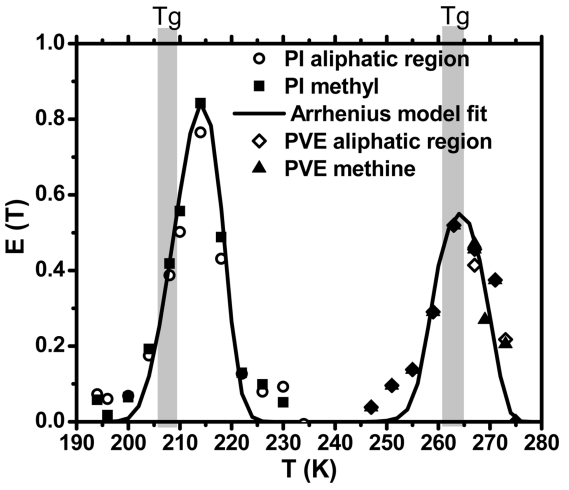

Figure 3. Normalized 200 ms exchange intensity **E**(**T**) curves for the total aliphatic region integrated intensity versus only the CH_3 intensity for pure PI, and total aliphatic intensity versus backbone-CH only for PVE. The DSC value for the T_g range of the pure polymers is shown as a shaded region. The solid lines are fits to the data using an Arrhenius/log−Gaussian model described in the text.

interaction. Using a 0.2 s mixing time, the onset of detectable slow chain dynamics occurs at temperatures lower than the 10 K/min DSC T_g (indicated by the shaded vertical stripe) for each component. However, the same effective glass transition difference (50 K) is observed from the initial temperature at which exchange intensity exists. Since multiple signals arise from each polymer component, one chooses that signal from each polymer that provides the best resolution in the blend spectrum. Often, this can be a methyl group, so it is important to verify that the temperature-dependent CODEX response is the same for a pendant methyl as it is for the main chain carbons. Control experiments verify this is the case for PI, as shown by the open and closed symbols in

Figure 3. Specific methyl group dynamics are much too fast to influence the magnitude of the exchange intensity signal, since the CODEX experiment probes the much slower 1−1000 Hz frequency regime, and while we expected the agreement shown in Figure 3 based on previous polymer systems, it is important to run the control for each polymer. Therefore, we can confidently use the resolved methyl signal in the blend spectra as an accurate measure of slow PI main-chain segmental dynamics.

Close examination of the first two to three points in the low temperature region of the PVE exchange curve (245−255 K) reveals additional sub-T_g dynamic modes that we have not observed in our previous studies of completely aliphatic polyolefins, and which do not follow expected behavior for residual spin-diffusion contributions to exchange intensity.[19,38] Note that these points do not follow a simple monotonic intensity rise relative to the rest of the $E(T)$ curve. There is excellent agreement between the intensity extracted from the entire aliphatic backbone signal region versus that extracted from only the backbone methine for these three points (Figure 3). We assign this apparent premature exchange intensity gain to a neighboring group effect, since the olefinic PVE side group has a large chemical shift anisotropy and in addition, as a side chain is expected to exhibit sub-T_g dynamics prior to the onset of main-chain dynamics. Time-dependent modulation of the shielding environment (due to susceptibility anisotropy) for the directly bonded backbone methine carbon will occur even if there is no backbone chain motion during the mixing time, manifesting itself as a premature onset of detectable exchange intensity. This is confirmed by data analysis on the integrated exchange intensity for the olefinic $=CH_2$ signal over the 245−255 K temperature range, which mirrors that of the aliphatic backbone CH at the first three temperature points in the PVE E(T) curve (data not shown). Unfortunately, a complete exchange curve could not be constructed for the specific signals from the PVE olefinic side group, as initially anticipated, since the olefinic side-chain dynamics increase quickly and interfere with the coherent averaging from ^1H decoupling resulting in complete loss of side-chain signal intensity beginning at 260 K.[39]

Exchange Data for Polymers in the Miscible Blend: Model-Independent Conclusions. Advanced polymeric mixtures, including those with inorganic components, and particularly those composed of structurally disordered phases, require that the experimentalist understand the specific behavior of the components in that mixture in order to tailor properties and define applications for the total material. As stated in the introduction, many recent experiments in polymer blend science indicate that one can only assume limited information from the pure-component behaviors. Figure 4 illustrates the power of the experimental NMR approach described here to separately and quantitatively identify constituent chain behavior in mixed polymer systems, and is particularly advantageous for mixtures of amorphous polymers. The exchange intensities versus temperature for pure and blended components as measured directly from the CODEX experiment are shown, as well as fits to the raw data using Arrhenius and WLF models.

Figure 4 represents the outcome of three independent variable-temperature experiments; one each for the two pure polymers and a single experiment for the blend from which polymer specific exchange intensities were extracted at each temperature. Prior to any consideration of a quantitative model to fit the results, several important points may be discerned via simple inspection of the raw data in Figure 4, and comparing the response of the NMR signals in the CODEX

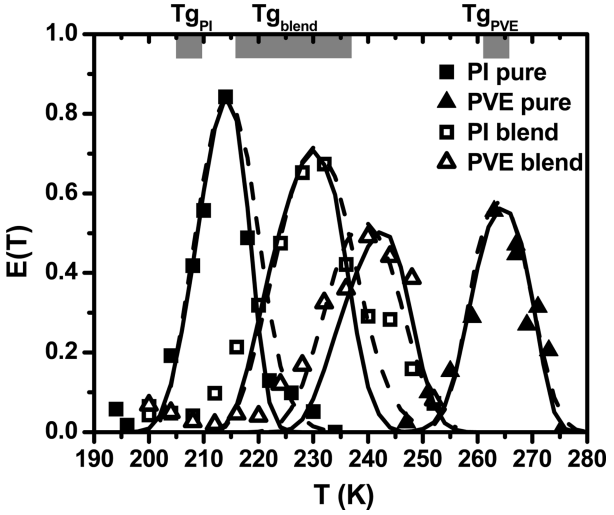

Figure 4. Normalized 200 ms exchange intensity $E(T)$ curves for the pure components and the same components measured independently in the blend. The solid lines are fits to the data using an Arrhenius model with a variable-width log−Gaussian correlation time distribution. The dashed lines are fits to the data using the WLF/KWW model. The thick gray lines at the top of the figure indicate the 10 K/min DSC T_g range for the two pure polymers and the miscible blend.

experiment for each pure polymer to the response of that same polymer in the blend. First, the onset of detectable exchange intensity occurs at temperatures at or below the calorimetric T_g, indicating that the 200 ms mixing time CODEX experiment is probing the slow segmental chain dynamics (i.e., conformational reorientations) operative during the glass transition. Second, the PI exchange intensity curve shifts to higher temperature in the blend relative to pure chains. Similarly, the exchange intensity curve shifts to lower temperature for the PVE in the blend compared to its pure response. For PI, the $E(T)$ maximum shifts from 214 to 230 K upon blend formation, while the PVE $E(T)$ maximum decreases from the pure value of 265 K to 240−243 K in the blend. The temperature shifts for the $E(T)$ curves of each component in the blend are not equivalent, nor do the curves converge to the same temperature range in Figure 4. The polymer components exhibit distinctly different glass transitions in the miscible blend. Third, the expected temperature to observe the maximum in each E(T) curve in the miscible blend, using Gordon−Taylor/Fox equations for composition weighted averaging, is 237 K. Neither blend component exhibits a maximum at this temperature; the PI maximum is 7−8 deg lower and the PVE maximum is 3−5 deg higher. Finally, the breadth of each $E(T)$ curve increases for either component in the blend relative to the pure polymer, clearly indicative of increased dynamic heterogeneity for blended versus pure polymers, in agreement with the observation that the absolute value of $E(T)$ at each temperature point across the detectable range decreases in the blend relative to the unmixed result for both polymer components (holding constant all other experimental parameters which could effect signal intensity). Interpretations of these direct inspection observations using quantitative physical models are presented the following sections.

Quantitative Segmental Dynamics for PI and PVE in the Miscible Blend. The fits to experimental data shown in Figures 3 and 4 were obtained using two different physical models. The $E(T)$ temperature dependence was analyzed by comparing an Arrhenius model using a discrete log−Gaussian correlation time distribution function to a WLF/KWW (Williams−Landel−Ferry/Kohlrausch−Williams−Watts) model. As we have previously discussed, an isotropic

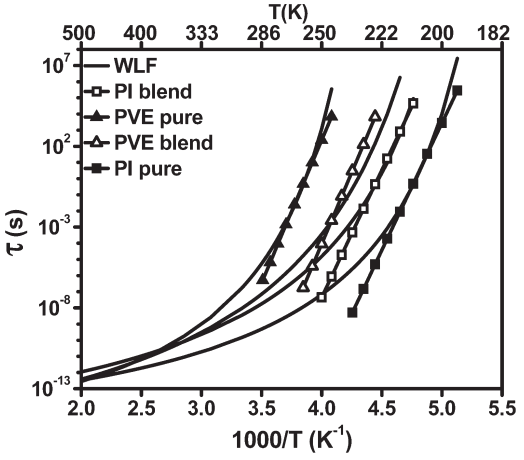

Figure 5. Temperature dependence of correlation times obtained using Arrhenius (points) and WLF (smooth line) models. The WLF parameters for pure PI were as follows: C_1 = 18.2, C_2 = 32 K, $\tau(T_g)$ = 10 000 s, and T_g = 200 K, whereas for PI in blend C_2 = 41 and T_g = 212 K was used. For pure PVE, C_1 = 19.2, C_2 = 42 K, $\tau(T_g)$ = 10 000 s, T_g = 248 K, and the best fit for PVE in the blend was obtained with C_2 = 48 K and T_g = 220 K. Note the close agreement for each model in the lower temperature regions consistent with segmental dynamics, but as expected, the Arrhenius fits diverge at high temperatures. In the WLF/KWW fits, the KWW β parameters for pure PI, blend PI, pure PVE, and blend PVE were 0.33, 0.33, 0.65, and 0.46, respectively.

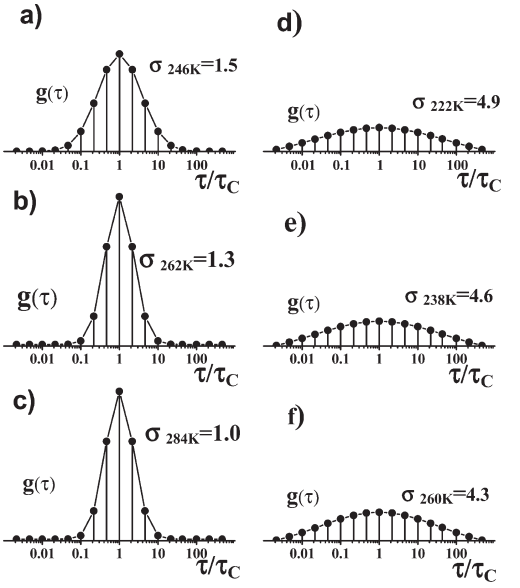

Figure 6. Example results for discrete versions of log-Gaussian correlation time distributions $g(\tau)$ for PVE, with different widths σ following a linear temperature dependence $\sigma(T) = ak_BT + \sigma_0$, at key temperatures spanning the $E(T)$ curve previously shown in Figure 4. Each distribution is centered at τ_c and consists of 17 points equally spaced over approximately 6 decades. Key: (a) pure PVE at 246 K, (b) pure PVE at 262 K, (c) pure PVE at 284 K, (d) PVE in blend at 222 K, (e) PVE in blend at 238 K, and (f) PVE in blend at 260 K.

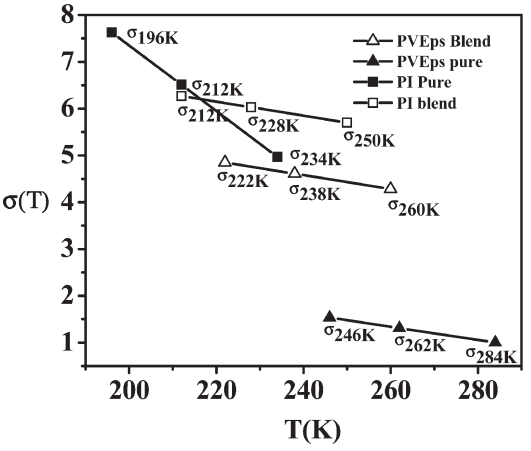

Figure 7. Temperature dependence of correlation time distribution widths σ for pure PI and pure PVE versus the same polymers in the blend, obtained using the Arrhenius/log-Gaussian model with linear temperature dependence for σ as explained in the text. Note the disparate slope for the pure components, but essentially identical slopes for the blended polymers, and the much larger change in the absolute values of σ for the high-T_g PVE blend component.

rotational diffusion model (employing 20 discrete conformer populations as an approximation to the heterogeneous backbone conformer distribution, and the small angle jumps between them) was used to simulate the experimental data and solve the overall equilibrium exchange matrix as a function of the exchange mixing time in the CODEX experiment and the correlation time constant for specific polymers at each temperature.[15−17] Figure 4 shows the results of each approach, indicated by solid versus dashed lines, respectively. Complete details for the calculations, as well as comparisons to other possible approaches cited in the literature, are provided in the Supporting Information. Extensive discussions of the data analysis steps for static (i.e., non-MAS) versions of this experimental approach may be found in refs 38 and 40.

The absolute value of the exchange intensity $E(T)$ at each temperature, for a fixed recoupling and exchange mixing time, depends on the correlation time constant characteristic of the motion modulating the chemical shift anisotropy as well as the distribution of correlation time constants for all of the segments in the amorphous polymer or polymer mixture (see Supporting Information). Figure 5 shows calculated results for the temperature dependence of the central correlation time constant, i.e., the characteristic time constant at center of distribution, obtained using both the Arrhenius/log−Gaussian and WLF/KWW models. As expected, the Arrhenius model breaks down at high temperatures for macromolecules, but over the majority of the temperature range relevant for slow segmental dynamics used in this study, the model is physically reasonable and contains fewer parameters and assumptions than the WLF/KWW approach. The sole purpose of the discrete points in Figure 5 are to indicate the temperatures at which raw exchange intensity data was obtained (Figure 4), and the straight lines through those points are the results of the Arrhenius fits. Figure 6 shows example calculated correlation time distributions obtained in the fitting process to the data in Figures 4 and 5 for the PVE component.

Figure 6 indicates that a large change in the PVE correlation time distribution width occurs once the miscible blend is formed, and also that the temperature dependence of the distribution is suppressed. Examination of the exchange intensity equations in the Supporting Information reveals how the magnitude of the distributions shown in Figure 6 can influence each point in the E(T) curves. Similar plots to those shown in Figure 6 could also be constructed for PI. A complete comparison of the behavior of both PI and PVE are summarized by Figure 7, in which the σ values from the full $g(\tau)$ expression are plotted versus temperature.

Figure 7 indicates that pure PI and pure PVE have much different temperature dependent slopes, and also shows the large effect blend formation has on the dynamic heterogeneity characterizing segmental dynamics for each

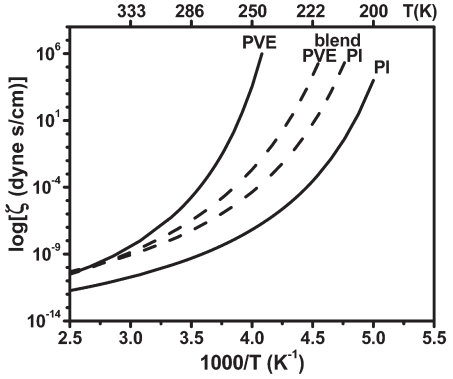

Figure 8. Calculated segmental friction coefficients using the central correlation time constants τ_c obtained from the WLF/KWW model fits to the CODEX exchange intensity data in Figure 4. The relationship $\zeta = \tau_c k_B T/b^2$ was used for the calculations, where $b = 1.1$ nm is the characteristic segment length for reorientation. The temperature range for the experimental data used to generate the curves is 196−286 K.

component. In particular, the high-T_g PVE component exhibits a significantly larger change in absolute value of σ in the blend relative to its pure component values, but preserves its slope. Conversely, the PI shows a relatively small change in the absolute value of σ at any temperature over the temperature range of interest, but a much larger change in its slope. Systematic comparison of σ's in the log-Gaussian model to KWW β parameters are discussed in support of Figure 4S of the Supporting Information.

Friction coefficients for chain segmental dynamics, as referenced to a specific length or chain subunit, may be obtained via direct diffusion measurements,[28] or calculated based on measured correlation time constants characteristic of that motion.[41] Direct experimental measurement of chain diffusion for high molecular weight polymers in bulk at temperatures near T_g is difficult, even via pulsed-field gradient methods, since the self-diffusion coefficients are too small. Figure 8 shows calculated friction coefficients ζ obtained from our experimental τ_c data, using the simple relationship $\zeta = \tau_c k_B T/b^2$, where $b = 1$ nm. Since the chemical shift anisotropy modulation giving rise to finite intensity in the $E(T)$ curves originates from slow segmental dynamics involving chain subunits, e.g. conformational reorientation, we do not scale the equation by molecular weight dependent terms as in a typical Rouse relaxation time model.

There is some uncertainty in the literature on the magnitude of the characteristic segmental reorientation/diffusion length for amorphous polymers, with most published reports espousing values between 1 and 3 nm. The CODEX experiment probes changes in chemical shielding arising from local conformational changes of chain subunits, and given that we are interpreting our data in the context of a rotational isotropic diffusion model (appropriate for amorphous materials), we have used a value at the lower end of the range of reported values, i.e., 1 nm, for the friction coefficient calculation.

Comparison with Previously Published Data. The PI/PVE blend system, as discussed earlier, is a well-studied system by a large variety of experimental and theoretical methods. Recently, Haley and co-workers have summarized experimental results from their own work on PI/PVE blends and also compared their results to those previously published by other groups.[28] In Table 2, we reference those contributions, and compare selected values of the central correlation time constant τ_c extracted from a summary figure in ref 28 to our values obtained in this study, for 50/50 PI/PVE blends. Inspection of Table 2 reveals close agreement between values

Table 2. Comparison of Literature Data Previously Summarized in Reference 28 with Experimental Results in This Contribution for 50/50 PI/PVE Blends

polymer	temperature (K)	literature τ_c (s)	experimental/ fit τ_c (s)
PI pure	222	2.0×10^{-4}	5.0×10^{-4}
PI pure	250	2.0×10^{-7}	1.0×10^{-7}
PI pure	286	5.0×10^{-9}	0.8×10^{-9}
PI blend	222	0.1	1.0
PI blend	250	0.5×10^{-5}	2.0×10^{-5}
PI blend	333	3.0×10^{-10}	3.0×10^{-10}
PVE pure	286	0.5×10^{-5}	1.0×10^{-5}
PVE pure	333	7.0×10^{-8}	2.0×10^{-8}
PVE blend	235	5.0	2.0
PVE blend	250	40.0×10^{-4}	6.0×10^{-4}

for each of the pure polymers, as well as their individual values in the miscible blends. We do not expect exact agreement, as the WLF/KWW and Arrhenius/log-Gaussian models we use here differ from the models used in the referenced work.[28,34,35] For example, Haley and co-workers used VTF models to fit experimental data, and the WLF fits used by Kornfield and co-workers employed different fitting parameters, most notably the value of the correlation time constant at the glass transition (much smaller than the $\tau T_g = 10\,000$ s that we use here), and the T_g values for the polymers in the blend. Here, we use the raw CODEX data to assign T_g's in the blend, and there are no temperature shifts of the individual data points plotted in Figure 5 or 8. Given the large number of models pervasive in the polymer literature and the variation in fitting parameters often used within the same models, as well as small but random temperature errors in the collection of raw data by various methods, Table 2 illustrates that the experimental results obtained here are within expected agreement with previously published results on a point by point basis. More importantly, the experimentally detected changes that occur for pure versus blended polymer components, as shown in Figures 5 and 8, are in excellent agreement with these previously published results.

Comparison of Correlation Time Constants Obtained from CODEX Data Analysis to Discrete Variable Mixing Time Experiments. To further validate that data obtained from the analysis of the CODEX data as a function of temperature are accurate, we compare segmental correlation time constants obtained from the temperature-dependent analysis of CODEX exchange intensity curves, like those shown in Figure 4, with the time constant for the exchange intensity as a function of mixing time, at the same temperature, obtained in separate variable mixing time experiments. Figure 9 shows the exchange intensity as a function of mixing time for four different pure polymers including PVE, atactic polypropylene (PP), head-to-head polypropylene (hhPP), and polyisobutylene (PIB) at the indicated temperatures. The correlation time constants, extracted from an exponential fit to the rising intensity curve, are indicated on each of the parts (a−d) in Figure 9. (In figures where there are multiple data points, either multiple carbon positions in the polymer chain were probed or, as in Figure 9d, two different recoupling times in the CODEX experiment were compared.) The results in Figure 9 indicate that the correlation time constants obtained by full analysis of the raw data in Figure 4 are accurate, with the largest difference for the polymers shown equal to 12% for PVE, and less in the other three cases. While the time required to generate the experimental data in Figure 4 is not trivial, such an approach is significantly shorter (by a factor of 5 to 10) than the time required to obtain full variable mixing time exchange curves, like those shown in Figure 9, over the entire temperature range used in Figure 4.

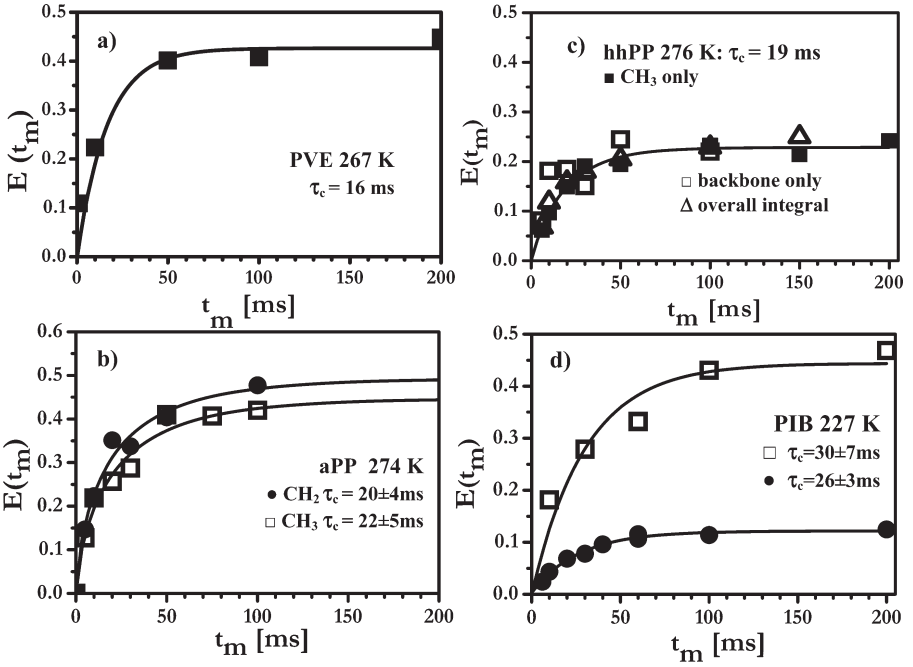

Figure 9. Exchange time constants extracted from an exponential fit to the rising exchange intensity curves are indicated on each part of Figure 9a−d for PVE, atactic PP (PP), head-to-head PP (hhPP), and polyisobutylene (PIB), respectively. For each of these same four polymers, at the same temperature as indicated on each plot, the respective central correlation time constants obtained from full analysis of the variable temperature exchange intensity curves of the type represented by the data in Figures 4 and 5, are (a) $\boldsymbol{\tau_c}$ = 14 ms, (b) $\boldsymbol{\tau_c}$ = 24 ms, (c) $\boldsymbol{\tau_c}$ = 20 ms, and (d) $\boldsymbol{\tau_c}$ = 25 ms. The temperatures indicated in parts a−d are equal or very nearly equal to the exchange intensity maximum temperature for each polymer, resulting in similar values of $\boldsymbol{\tau_c}$.

Conclusions

A chain-specific experimental approach based on variable-temperature solid-state CODEX NMR experiments reveals that the effective glass transitions for each chain type in PI/PVE blends are inequivalent, and slow segmental dynamics for each polymer in the blend are characterized by unique central correlation times and unique correlation time distributions. Quantitative analyses of the raw data indicate that good agreement exists between effective T_g's, central correlation time constants, correlation time distributions, and friction coefficients extracted from this approach versus those obtained by other well-documented methods. Results from an isotropic rotation diffusion model with Arrhenius/log−Gaussian or WLF/KWW treatments of temperature dependence show clear sensitivity to changes that occur upon blend formation relative to the unmixed components. That such quantitative information may be obtained for either polymer component in an amorphous mixture, without isotopic labeling, electric dipole moment constraints, or introduction of probe molecules, is a unique advantage of this experimental strategy and illustrates applicability to a wide range of mixed macromolecular systems beyond miscible blends, including polymer nanocomposites, organic/inorganic hybrids, biological macromolecules, and block copolymers.

Acknowledgment. The authors gratefully acknowledge support from the National Science Foundation Division of Materials Research through Grant DMR-0756291.

Supporting Information Available: Text giving the theoretical calculation of normalized exchange intensity, exchange matrix for isotropic rotational diffusion model, matrix of initial populations in isotropic rotational diffusion model, matrix of NMR frequencies, distribution of correlation times and figures showing plots of mean correlation time, plots of discrete 17-points KWW distribution, and the relationship between β_{KWW} parameter of KWW distribution and half-height width of log−Gaussian distribution. This material is available free of charge via the Internet at http://pubs.acs.org.

References and Notes

(1) Richert, R. *J. Phys.: Condens. Matter* **2002**, *14*, R703.
(2) Cangialosi, D.; Colmonero, J. *Phys. Rev. E* **2009**, *80*, 041505.
(3) Lodge, T. P.; Wood, E. R.; Haley, J. C. *J. Polym. Sci. B, Polym. Phys.* **2006**, *44*, 756.
(4) Gaikwad, A. N.; Wood, E. R.; Ngai, T.; Lodge, T. P. *Macromolecules* **2008**, *41*, 2502.
(5) Paul., W.; Smith, G. D. *Rep. Prog. Phys.* **2004**, *67*, 1117.
(6) Ediger, M. D. *Annu. Rev. Phys. Chem.* **2000**, *51*, 99–128.
(7) Lodge, T. P.; McLeish, T. C. B. *Macromolecules* **2000**, *33*, 5278.
(8) Liu, W.; Bedrov, D.; Kumar, S. K.; Veytsman, B.; Colby, R. H. *Phys. Rev. Lett.* **2009**, *103*, 037801.
(9) Milner, S. T.; McLeish, T. C. B. *Phys. Rev. Lett.* **1998**, *81*, 725.
(10) Kumar, S. K.; Shenogin, S.; Colby, R. H. *Macromolecules* **2007**, *40*, 5759.
(11) Haley, J. C.; Lodge, T. P. *Colloid Polym. Sci.* **2004**, *82*, 793.
(12) Painter, P.; Coleman, M. *Macromolecules* **2009**, *42*, 820.
(13) Colmenero, J.; Arbe, A. *Soft Matter* **2007**, *3*, 1474.
(14) Wolak, J. E.; Jia, X.; White, J. L. *J. Am. Chem. Soc.* **2003**, *125*, 13660.
(15) Wachowicz, M.; White, J. L. *Macromolecules* **2007**, *40*, 5433.
(16) Wachowicz, M.; Wolak, J. E.; Gill, L.; White, J. L. *Macromolecules* **2008**, *41*, 2832.
(17) Wachowicz, M.; Gill, L.; White, J. L. *Macromolecules* **2009**, *42*, 553.
(18) deAzevedo, E.; Hu, W. G.; Bonagamba, T. J.; Schmidt-Rohr, K. *J. Am. Chem. Soc.* **1999**, *121*, 8411–8412.
(19) deAzevedo, E.; Hu, W. G.; Bonagamba, T. J.; Schmidt-Rohr, K. *J. Chem. Phys.* **2000**, *112*, 8988–9001.
(20) Hefner, S.; Mirau, P. A. *Macromolecules* **1994**, *27*, 7283.
(21) Roovers, J.; Toporowski, P. M. *Macromolecules* **1992**, *25*, 1096.
(22) Roovers, J.; Toporowski, P. M. *Macromolecules* **1992**, *25*, 3454.
(23) Alegria, A.; Colmonero, J.; Ngai, K. L.; Roland, C. M. *Macromolecules* **1994**, *27*, 4486.
(24) Haley, J. C.; Lodge, T. P. *J. Rheol.* **2005**, *49*, 1277.
(25) Min, B.; Qiu, X.; Ediger, M. D.; Pitsikalis, M.; Hadjichristidis, N. *Macromolecules* **2001**, *34*, 4466.

(26) Cangialosi, D.; Alegria, A.; Colmonero, J. *Macromolecules* **2006**, *39*, 7149.
(27) Sakaguchi, T.; Taniguchi, N.; Urakawa, O.; Adachi, K. *Macromolecules* **2005**, *38*, 422.
(28) Haley, J. C.; Lodge, T. P.; He, Y.; Ediger, M. D.; von Meerwall, E. D.; Mijovic, J. *Macromolecules* **2003**, *36*, 6142.
(29) Kamath, S.; Colby, R. H.; Kumar, S. K.; Karastos, K.; Floudas, G.; Fytas, G.; Roovers, J. L. *J. Chem. Phys.* **1999**, *111*, 6121.
(30) Trask, C. A.; Roland, C. M. *Macromolecules* **1989**, *22*, 256.
(31) Bahani, M.; Laupretre, F.; Monnerie, L. *J. Polym. Sci. B, Polym. Phys.* **1995**, *33*, 167.
(32) Colby, R. H.; Lipson, J. E. G. *Macromolecules* **2005**, *38*, 4919.
(33) Ambler, M. R. *J. Appl. Polym. Sci.* **2008**, *109*, 2029.
(34) Chung, G. C.; Kornfield, J. A.; Smith, S. D. *Macromolecules* **1994**, *27*, 964.
(35) Chung, G. C.; Kornfield, J. A.; Smith, S. D. *Macromolecules* **1994**, *27*, 5729.
(36) Saxena, S.; Cizmeciyan, D.; Kornfield, J. A. *Solid State Nucl. Magn. Reson.* **1998**, *12*, 165.
(37) Fetters, L. J.; Lohse, D. J.; Colby, R. H. In *Physical Properties of Polymers Handbook*; Mark, J. E., Ed.; Springer: New York, 2007; p 447.
(38) deAzevedo, E. R.; Tozoni, J. R.; Schmidt-Rohr, K.; Bonagamba, T. J. *J. Chem. Phys.* **2005**, *122*, 154506.
(39) Rothwell, W. P.; Waugh, J. S. *J. Chem. Phys.* **1981**, *74*, 2721–2732.
(40) Kaufmann, S.; Wefing, S.; Schaefer, D.; Spiess, H. W. *J. Chem. Phys.* **1990**, *93*, 197–214.
(41) Rubenstein, M.; Colby, R. H. *Polymer Physics*; Oxford University Press: New York, 2003.